Developing Flow of a Gas-Particle Mixture in a Vertical Riser

Jorge A. Pita
Mobil Research and Development Corp., Paulsboro, NJ 08066

Sankaran Sundaresan
Dept. of Chemical Engineering, Princeton University, Princeton, NJ 08544

A computational study of steady, developing flow of gas-particle suspensions in a vertical riser has been carried out, using a model based on kinetic theory of granular materials, to understand the role of inlet configuration on the pattern of flow development. Three inlet configurations—uniform inlet, core-annulus flow at the inlet and circumferential injection of secondary gas—were examined. It is found that the inlet configuration can have a profound impact on the rate of segregation of particles to the wall and the internal recirculation. Circumferential injection of gas has a favorable effect on the flow in the sense that it can decrease the extent of internal recirculation.

Introduction

Circulation of particulate materials within processing facilities using a gas as the carrier fluid is frequently encountered in industrial practice (Yerushalmi and Avidan, 1985). The direction of solids flow may be vertically upward as in risers, vertically downward as in standpipes, or through ducts of intermediate inclination. When the axis of the pipe is not vertical, it is clear that the particles will be distributed nonuniformly over the cross section as a result of gravitational sedimentation, so one-dimensional theoretical treatments are inappropriate. Marked segregation of the particles over the cross section, however, occurs even in vertical flow (Bartholomew and Casagrande, 1957; Saxton and Worley, 1970; Yerushalmi et al., 1978; Youchou and Kwauk, 1980; Weinstein et al., 1984; Bader et al., 1988). In some cases, they are found to be concentrated near the pipe wall, while in others large regions of high concentrations, called streamers, extend well into the center of the pipe. As a consequence of this, one-dimensional theoretical models have been unsuccessful in making quantitative predictions without the injection of empiricism in the form of fitted parameter values which depend on the nature of the particles and the size of the pipe (Hinze, 1962; Gidaspow and Solbrig, 1976; Arastoopour and Gidaspow, 1979a,b; Arastoopour et al., 1982; Arastoopour and Cutchen, 1985; Adewani and Arastoopour, 1986; Leung and Jones, 1978; Ginestra et al., 1980; Chen et al., 1984; Mountziaris and Jackson, 1990).

The primary large-scale mechanical effect of lateral segregation over the cross section is to generate cross-sectional average values of the slip velocity between particles and gas, which greatly exceeds the local slip anywhere in the pipe. However, the detailed form of the particle concentration profile is also important, since it influences the distribution of residence times of particles within any given section of the duct and may even generate recirculation of particles against the direction of set flow. These effects are of critical importance in predicting the behavior of systems in which the particles react chemically with the gas or catalyze a reaction between substances present in the gas. For example, the riser reactors used for the catalytic cracking of gas oil use a transported solid catalyst, and their performance can be predicted with confidence only if the physical mechanism that determines the cross-sectional distribution of the catalyst can be identified and modeled.

Possible causes for the occurrence of the lateral segregation of solids over the cross section have been explained effectively by Sinclair and Jackson (1989). They point out that in the motion of a gaseous suspension both the fluid and particle velocities will have local average and random components and that the interaction of the fluctuating part of the particle motion with the mean particle motion will generate stresses in the particle assembly. They constructed a mathematical model for fully-developed flows in vertical pipes taking into account this particle-phase interaction (and neglecting the effect of gas-phase turbulence). As the kinetic energy of the random motion of particles is analogous to that of the thermal motion of molecules in a gas, it can be characterized by a "granular temperature" proportional to the mean square of the random component of the particle velocity. The particle velocity fluctuations generate an effective pressure in the particle phase, together with an effective viscosity which resists shearing of the particle assembly. Both the effective pressure and the effective viscosity depend strongly on the granular temperature, so this must be found by solution of a separate differential equation representing a balance for the pseudothermal energy of random motion of the particles. Pseudothermal energy is generated by the working of the effective shear stresses in the particle phase, dissipated by the inelasticity of collisions between particles, and conducted from place to place as a result of gradients in the granular temperature. Thus, a fully developed flow is generated by solving simultaneously three coupled ordinary differential equations, representing force balances for the gas and particle phases, and a conservation equation for the pseudothermal energy of the random component of particle motion.

This model revealed a remarkably rich variety of behavior over the whole range of possible flow conditions: cocurrent upflow, cocurrent downflow, and countercurrent flow (Sinclair and Jackson, 1989). Particle concentration was found to be high near the wall of the duct; depending on the elastic properties of particle-particle and particle-wall collisions, it could also be high near the axis of the tube. Particle recirculation was also observed in some situations, and choking and flooding phenomena were indicated.

In an earlier publication (Pita and Sundaresan, 1991), we examined the scaleup characteristics predicted by this model and compared the model with experimental data. It was found that the model predicted some of the experimental data in an almost quantitative fashion, provided that the damping of the random component of particle motion by inelastic particle-particle collisions and gas drag were ignored. The model did, however, manifest an unsatisfactory degree of sensitivity to these dampings.

Louge et al. (1991) have expanded the above model to account for the effect of gas-phase turbulence; however, it appears that the particle-particle interaction is the key element required to produce lateral segregation of solids. Ding and Gidaspow (1990) and Tsuo and Gidaspow (1990) have carried out numerical integration of transient two-phase flow in a vertical slit and demonstrated that the flow patterns observed in the simulations were qualitatively similar to those recorded experimentally. It is also clear from their study that the transient integration did not converge toward any steady state; instead, the fluctuations persisted even after long periods of time. This is certainly consistent with experimentally observed trends, at least in a qualitative sense. Their study is particularly valuable as it demonstrated that the essential features of gas-particle flow can indeed be captured by solving the continuity and the momentum balance equations for the two phases, and the pseudothermal energy balance equation.

Transient integration of the conservation equations requires large computational times, and hence it is not practical to carry out a large number of simulations over a wide range of operating conditions. Furthermore, the underlying attractors to which the transient solutions are evolving cannot be seen clearly from these simulations. Finally, as their simulations are only two-dimensional, the statistical data on fluctuations gathered from these simulations cannot be compared with experimental data, thus limiting the usefulness of the transient results. These considerations prompted us to undertake the present study in which we have computed the steady, developing flow of gas-particle suspensions in vertical pipes predicted by this model. Through such computations we have examined the entrance and exit effects, evolution of internal recirculation, and some scaleup issues associated with gas-particle flows in risers.

Mathematical Model

The volume-averaged equations of motion for the steady, developing flow of a gas-particle mixture are as follows (Anderson and Jackson, 1967):

Continuity:

$$\nabla \cdot (\rho_i \epsilon_i \underline{U}_i) = 0, \quad i = s, g \tag{1}$$

Momentum balance:

$$\nabla \cdot (\rho_g \epsilon_g \underline{U}_g \underline{U}_g) = -\epsilon_g \nabla P + \epsilon_g \rho_g \underline{g} + \beta_{sg}(\underline{U}_s - \underline{U}_g) \tag{2}$$

$$\nabla \cdot (\rho_s \epsilon_s \underline{U}_s \underline{U}_s) = -\epsilon_s \nabla P + \epsilon_s \rho_s \underline{g} + \beta_{sg}(\underline{U}_g - \underline{U}_s) - \nabla \cdot \underline{\underline{\sigma}} \tag{3}$$

where

$\underline{U}_g$, $\underline{U}_s$ = local average velocity of gas and particles, respectively
P = gas-phase pressure
σ_{ij} = components of the stress tensor associated with the particle assembly, defined compressively
ρ_g, ρ_s = density of gas and solid, respectively
ϵ_g, ϵ_s = local average volume fraction of gas and solid, respectively ($\epsilon_g + \epsilon_s = 1$)
$\underline{g}$ = acceleration due to gravity
$\beta_{sg}(\underline{U}_s - \underline{U}_g)$ = drag force per unit total volume exerted between the phases

In the above equations, we have neglected the deviatoric (volume-averaged) stress in the gas phase. We found in an earlier study (Pita and Sundaresan, 1991) that these deviatoric stresses are indeed negligible in gas-particle flows in the so-called fast fluidization regime of flow where industrial risers operate.

Pseudothermal energy balance:

$$\frac{3}{2} \nabla \cdot (\epsilon_s \rho_s \underline{U}_s \theta) = -\nabla \cdot \underline{q}_{pt} - \underline{\underline{\sigma}} : \nabla \underline{U}_s - \gamma_1 - \gamma_2 \tag{4}$$

θ = granular (or particle) temperature
$\underline{q}_{pt}$ = pseudothermal energy flux due to a "conductive" process
γ_1, γ_2 = dissipation of pseudothermal energy by inelastic collisions between particles and gas-particle drag, respectively

The terms appearing in the pseudothermal energy balance equation are described in detail by Lun and Savage (1984), Johnson and Jackson (1987), and Ding and Gidaspow (1990). To close the above set of equations, constitutive relations are needed for the particle-phase stress ($\underline{\underline{\sigma}}$), the pseudothermal energy flux ($\underline{q}_{pt}$), the rates of dissipation of pseudothermal energy (γ_1 and γ_2), and the interphase drag coefficient (β_{sg}). For the first three, we use slightly modified forms of the expressions derived by Lun and Savage (1984). For the fourth and fifth, we adopt expressions suggested in Ding and Gidaspow (1990).

$$\underline{\underline{\sigma}} = \rho_s \epsilon_s \theta (1 + 4\epsilon_s g_o) - \mu_b [\nabla \cdot \underline{U}_s] \underline{\underline{I}} - 2 f_1 \underline{\underline{S}}$$

$$2\underline{\underline{S}} = (\nabla \underline{U}_s + \nabla \underline{U}_s^T) - \frac{2}{3} (\nabla \cdot \underline{U}_s) \underline{\underline{I}} \tag{5}$$

$$\underline{q}_{pt} = -f_2 \nabla \theta \tag{6}$$

$$\gamma_1 = \frac{48\eta}{\sqrt{\pi}} (1-\eta) \frac{\rho_s \epsilon_s^2}{d_s} g_o \theta^{3/2} \tag{7}$$

$$f_1 = \frac{\mu}{g_o} \left(1 + \frac{8}{5} \epsilon_s g_o\right)^2 + \frac{3}{5} \mu_b \tag{8}$$

$$f_2 = \frac{\lambda}{g_o} \left[\left(1 + \frac{12}{5} \epsilon_s g_o\right)^2 + \frac{512}{25\pi} \epsilon_s^2 g_o^2 \right] \tag{9}$$

$$\beta_{sg} = \frac{3}{4} C_d \frac{\epsilon_g \epsilon_s \rho_s |\underline{U}_g - \underline{U}_s|}{d_s} \cdot \epsilon_g^{-2.65} \tag{10}$$

$$\gamma_2 = 3\beta_{sg}\theta \tag{11}$$

where

$$\mu = 5m(\theta/\pi)^{1/2}/16 d_s^2; \quad \mu_b = 256 \mu \epsilon_s^2 g_o / 5\pi$$

$$\eta = (1+e)/2; \quad \lambda = 75 m (\theta/\pi)^{1/2} / 64 d_s^2$$

$$g_o = (1 - (\epsilon_s/\epsilon_o)^{1/3})^{-1} \quad \text{and}$$

$$C_d = \begin{cases} 24(1 + 0.15 Re_g^{0.687})/Re_g & \text{if } Re_g < 10^3 \\ 0.44 & \text{if } Re_g > 10^3 \end{cases} \tag{12}$$

with Re_g defined as:

$$Re_g = \epsilon_g \rho_g |\underline{U}_g - \underline{U}_s| d_s / \mu_g$$

In the above equations, m is the mass of a particle, d_s is particle diameter, e is the coefficient of restitution for collisions between particles, ϵ_o is the particle volume fraction at close-packing, and $\underline{\underline{I}}$ is the identity tensor. In the formulation of Lun and Savage (1984), $\underline{\underline{\sigma}}$ was a function of η and gradients in volume fraction as well. As pointed out by these authors, however, the term proportional to volume fraction gradient is of higher order than the term proportional to the gradient in granular temperature. Taking $(1-e)$ to be a small parameter and retaining only the first-order terms as suggested by Jenkins (1987), one obtains the constitutive relations described above.

Riser Geometry

In this study, we have restricted our attention to a special geometry of the riser so that we can assume cylindrical symmetry. Accordingly, we will consider a vertical cylindrical tube of radius R_t. Both inlet and exit configurations will be so chosen to preserve the validity of assumed symmetry. In all the cases discussed in this article, it is assumed that the gas and solid exit the riser (at the top) in the radial direction. Three different inlet configurations were studied, as shown in Figure 1.

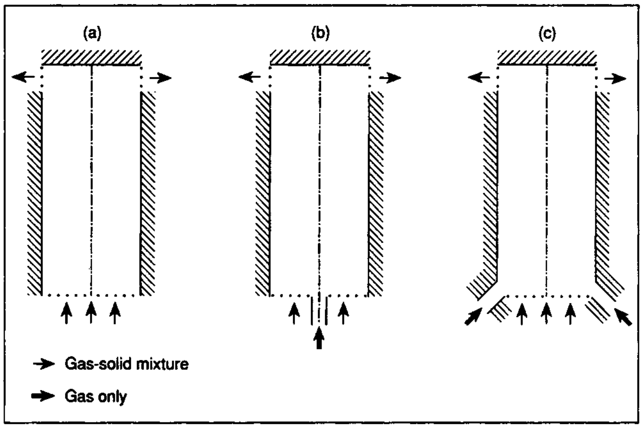

Figure 1. Riser configurations.

Case a. Figure 1a describes schematically the case of *uniform inlet* at the bottom. The walls of the riser (not available for inflow or outflow) are shown by solid lines. The inlet and exit are shown as broken lines. In this case of uniform inlet, it is assumed that the volume fraction of particles, gas and particles (axial) velocities, and the granular temperature in the entering stream are radially uniform.

Case b. Figure 1b describes the case of a *core-annulus flow* at the bottom inlet. Here, a mixture of gas and solid enters in the annular region ($R_o < r < R_t$), and a stream of gas is added in the core region. It is assumed that the volume fraction of solid, gas and particle (axial) velocities and the granular temperature are (radially) uniform in the suspension entering in the annular region. It is further assumed that the gas entering the riser in the core region has no radial velocity component.

Case c. Figure 1c describes another case of dual inlet, namely, *circumferential gas injection*. Here, a uniform inflow of gas and particles occurs at the bottom of the riser as in case a. In this case, however, we have an additional inflow of gas along the circumference. This case is an idealization of a large number of nozzles placed along the circumference by a continuous, ring-type inlet placed on the circumference. We have allowed this secondary gas stream to have both radial and axial velocity components. In other words, one can specify the angle of inclination of the nozzles.

The configurations described under cases b and c are indeed relevant in some commercial FCC risers. If we replace the secondary gas stream (added in the core in case b and circumferentially in case c) with liquid streams, we obtain almost realistic pictures of some FCC risers. It is of significant practical importance and thus the objective of this study is to understand how changes in the inlet configuration affect the evolution of gas and solid flow streamlines, and particle segregation in FCC (and other) risers.

Boundary Conditions

It is assumed that all the incoming streams are completely specified, that is, the volume fraction of solid, the gas and solid velocities, and the granular temperature for the incoming streams are given. At the outlet, pressure is specified. In addition, a continuation condition (Ding and Gidaspow, 1990) is used at the exit for granular temperature and solid volume fraction. The variation of radial velocities with radial coordinate at the exit then simply follows from continuity equations.

At the wall, the velocities of gas and particle normal to the surface were set to be zero. Two additional conditions, a shear stress balance at the wall for the particle phase, and a balance equation for the pseudothermal energy exchange were also imposed at the wall. These are exactly the same as those used by Hui et al. (1984), Sinclair and Jackson (1989), and Pita and Sundaresan (1991).

$$(\underline{I}-\underline{n}\ \underline{n})\cdot\underline{\underline{\sigma}}\cdot\underline{n}=\frac{\Phi^{1}\sqrt{3}\pi\rho_s\epsilon_s\theta\underline{U}_s g_o}{6\epsilon_o}$$

$$\underline{q}_{pt}\cdot\underline{n}=\frac{\sqrt{3}\pi\epsilon_s\rho_s\theta^{3/2}(1-e_w^2)g_o}{4\epsilon_o}-\underline{U}_s\cdot\underline{\underline{\sigma}}\cdot\underline{n}$$

where $\underline{n}$ is a vector normal to the surface; ϕ^1 is a specularity factor whose value ranges from zero, when collisions between particles and the wall are specular, to unity, when incident particles are scattered diffusely; and e_w is the coefficient of restitution for particle-wall collisions.

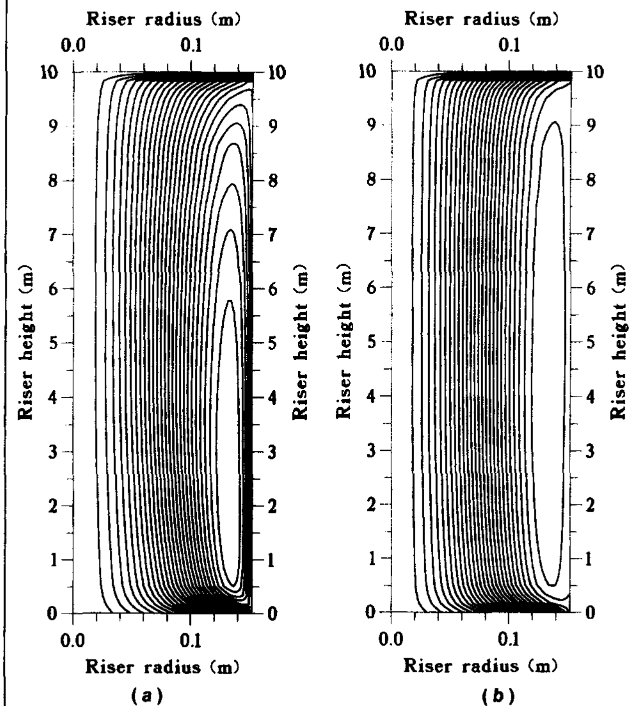

Figure 2. Streamlines: a. particle phase; b. gas phase.

See Tables 1 and 2 for parameter values; uniform inlet.

Computational Approach

The system of governing equations was discretized using finite differences with staggered grids. The continuity equations are written as mass conservations for each of the cells. To introduce the boundary conditions, fictitious cells were defined outside the domain of integration. The discretization procedure and the manner in which boundary conditions are brought into the analysis are exactly the same as those used by Ding and Gidaspow (1990) and Tsuo and Gidaspow (1990). The resulting set of nonlinear algebraic equations was solved by a damped Newton-Raphson method consisting of a linearization phase (that is, Jacobian generation) and a linear solution phase.

Computations were performed on an eight-processor Cray Y-MP using a FORTRAN77 autotasking compiler that enables parallelization of the computational load among different processors. Linearizations are performed in parallel so that the solids continuity equation can be handled by one processor concurrently with the gas continuity equation in another processor. The remaining processors are allocated, also concurrently, the tasks of linearizing the gas axial momentum, gas radial momentum, solids axial momentum, solids radial momentum, and the particle temperature equation. Once the linearization has been completed, linear solution of the system of equations is performed.

Parallel processing has little effect on total CPU time, but can drastically reduce the actual wall-clock time for the job. In terms of CPU time, a 60 × 30 grid simulation can take up to 6 Cray CPU minutes per Newton iteration. Depending on the system load, actual wall-clock time can become one-sixth of that amount. The total time for a simulation depends linearly on the number of Newtonian iterations required for convergence. These typically range from 10 to 50. A very tight tolerance was demanded for the continuity equations to assure mass conservation. As a further check on mass conservation, the inflows at the bottom of the riser were compared with the net upflow at various heights at the exit.

Results and Discussion

Uniform inlet

Let us first consider the case of uniform inlet conditions for both gas and particles at the bottom of the riser tube (case a mentioned earlier). We have used the case studied by Bader et al. (1988), henceforth referred to as IGT case, as the base case. Computational results have been generated for different bed heights, exit openings, inlet granular temperatures, and coefficient of restitution for particle-particle collisions to develop a physical picture of the model predictions. We will describe below the results obtained for eight different cases.

Figures 2a and 2b describe the solid-phase and gas-phase streamlines obtained with the base IGT case. The parameter values corresponding to this base case are listed in Tables 1

Table 1. Basic Simulation Parameters

Particle Diameter	76 μm
Particle Density	1,714 kg/m^3
Gas Density	1.22 kg/m^3
Gas Viscosity	4×10^{-5} kg/m·s
Particle-Particle Restitution Coefficient	1
Solids Volume Fraction Limit	0.65

Table 2. Uniform Inlet

Riser Height	10 m
Riser Radius	0.152 m
Radial Outlet (at the Top) Opening	0.1 m
Inlet Solids Volume Fraction	0.0218
Outlet Pressure	1.013×10^5 N/m^2
Inlet Solids Axial Velocity	2.62 m/s
Inlet Solids Radial Velocity	0
Inlet Gas Axial Velocity	3.78 m/s
Inlet Gas Radial Velocity	0
Inlet Particle Temperature	30 m^2/s^2

Table 3. Particle Residence Times

Fig. No.	Inventory of Particles in Bed		Residence Time (s)
	kg	Vol.%	
2	39.0	3.135	5.5
3	203.1	3.628	28.6
4	3.785	0.304	4.3
5A	30.8	2.476	4.34
5B	20.9	1.680	2.94
6	50.9	4.092	7.2
7	38.7	3.111	5.45
8	39.1	3.143	5.5
9	134.9	2.711	4.75
10	60.4	4.855	8.5
11	544.2	4.042	7.1
12	29.8	2.395	4.2
14	29.8	2.395	4.2

and 2. This corresponds to a riser gas superficial velocity of 3.86 m/s and a solids flux of 98 kg/m^2·s. The streamlines do start off vertically upward at the very bottom of the riser. But, they are rapidly deflected inward to the cylinder axis by the solids flowing downward in the wall region. Apparently, the riser is not tall enough to obtain a noticeably large "fully developed" region in the middle.

Figures 3a and 3b show the streamlines obtained with a 45-m-tall riser. A nearly "fully developed" region of flow can indeed be seen in this case. The radial and axial variations of solids fraction are shown in Figure 3c. The segregation of particles toward the wall region is clearly evident.

The total inventory of particles in the bed for the various cases examined in this study are presented in Table 3 along with the corresponding particle phase residence times. An increase in the riser height from 10 m to 45 m has increased the particle inventory by much more than a factor of 4.5. Fully developed flow calculations of the type described in our earlier

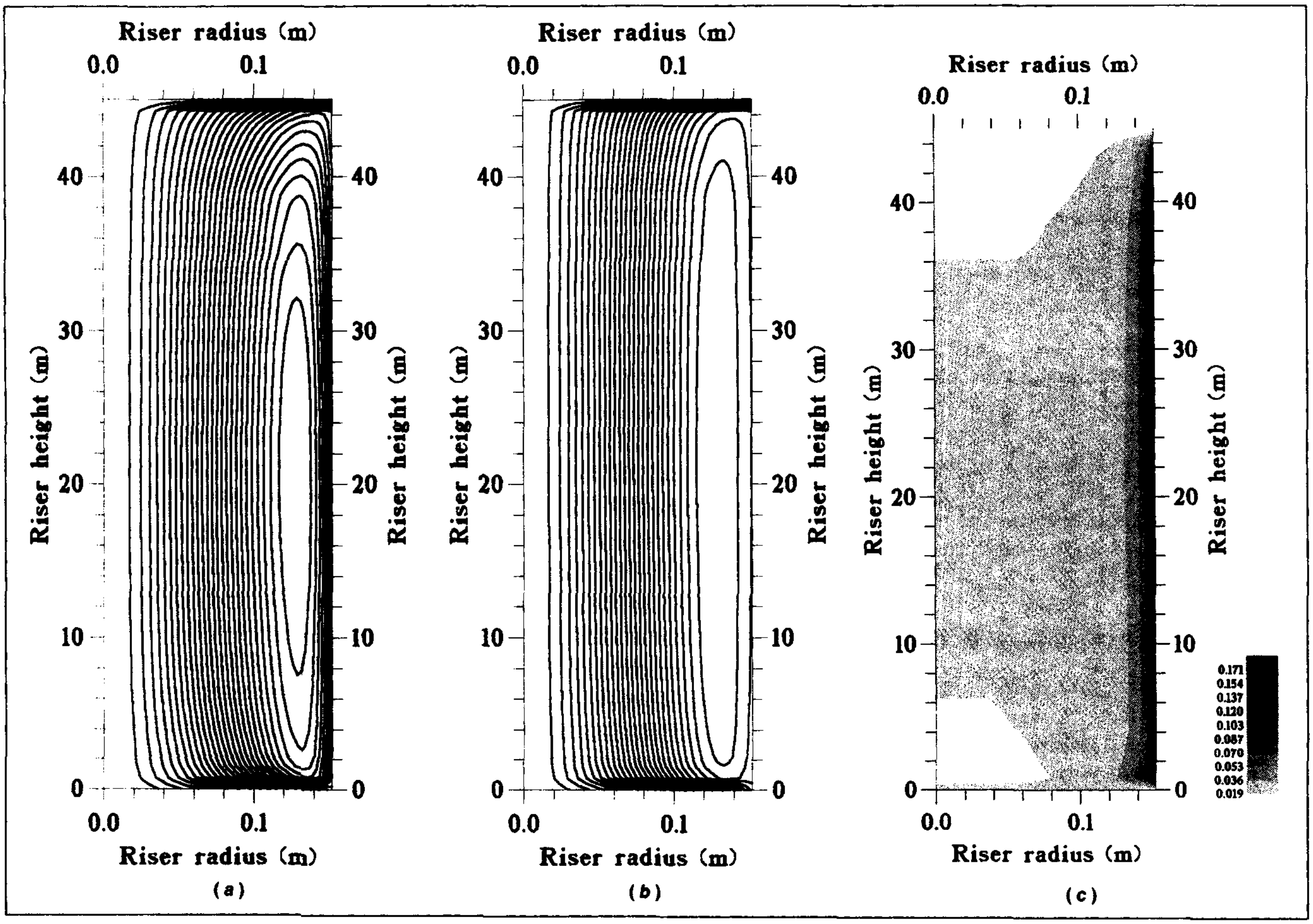

Figure 3. a. Particle-phase streamlines; b. gas-phase streamlines; c. spatial variation of solid fraction.
45-m-tall riser with uniform inlet.

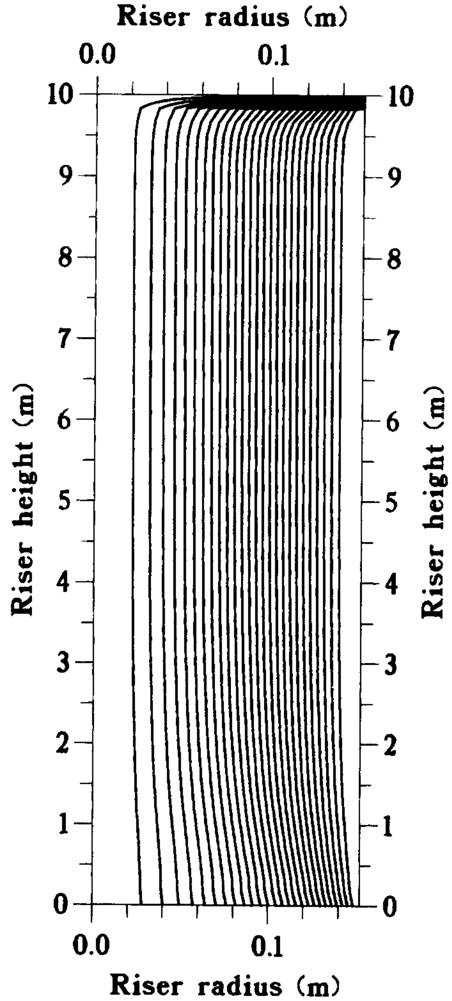

Figure 4. Particle-phase streamlines.

See Tables 1 and 2 for parameter values, but inlet solids axial velocity here equals 0.325 m/s.

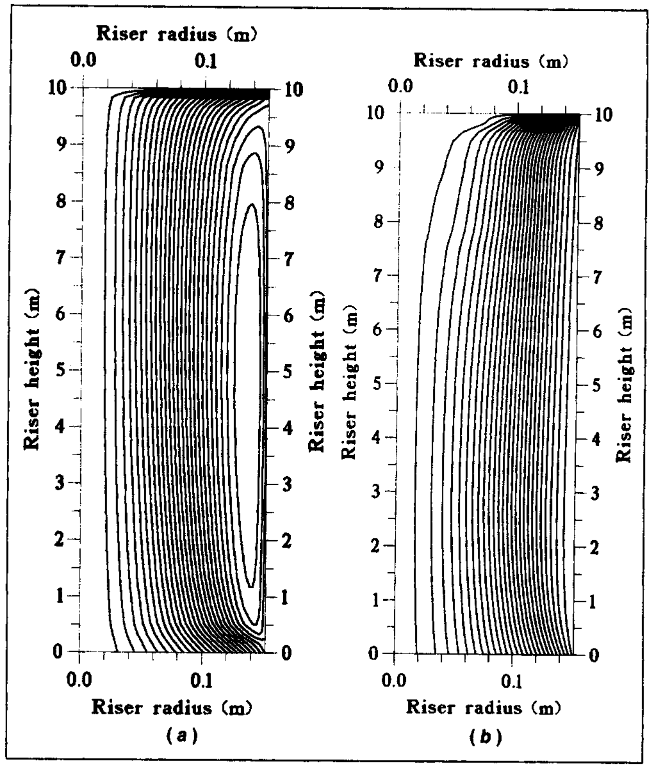

Figure 5. Particle-phase streamlines with inlet particle temperature of: a. 10 m^2/s^2; b. 1 m^2/s^2.

See Tables 1 and 2 for other parameter values.

publication (Pita and Sundaresan, 1991) reveal that the cross-sectional average-volume fraction of solids in the fully developed region for this combination of solids and gas fluxes, and model parameters is 0.047. Thus, the average-volume fraction of particles ($\langle\epsilon_s\rangle$) in the 45-m-tall riser is closer to the fully-developed value (see Table 3). The analysis predicts that $\langle\epsilon_s\rangle$ values for risers of finite height are smaller than the fully developed value.

Pattern of Flow Development

Figure 4 shows the streamlines obtained when the solid flux was reduced by a factor of 8, while keeping all other quantities as in Tables 1 and 2. Note that the solid flow streamlines in Figures 2a and 4 are deflected toward the tube axis upon entry into the riser, with the deflection being more pronounced in the former. It is straightforward to rationalize this trend. In both cases, upon entry into the riser, the particles in the wall region slow down. Consequently, the particles in the core region travel faster to conserve the flux, which shows up as a deflection of the streamlines toward the axis. (Such a trend would be obtained even in an incompressible, Newtonian fluid flow in a pipe). Note that in Figure 2a there is a downflow of particles in the wall region (away from the inlet), while there is no downflow in Figure 4. (Although there is no downflow in Figure 4, an appreciable segregation of particles toward the wall still occurs in this case.) This downflow of particles (Figure 2a) should necessarily lead to an increased deflection of the streamlines toward the tube axis. The elimination of internal recirculation of particles has led to a decrease in the residence time of particles in the column from 5.5 s (Figure 2A) to 4.3 s (Figure 4) (see Table 3). The average-volume fraction of solids in bed for the case described in Figure 4 is 0.00304, while that for a fully developed flow with identical fluxes is 0.0031. This suggests that the entrance and exit regions must be much smaller than 10 m for this case. It appears reasonable to conclude that if there is no flow recirculation in the fully developed state, the flow develops to this state rather quickly.

Effect of inlet granular temperature

While we can specify the volume fractions and velocities of the gas and solid phases at the inlet with confidence, little is known about the granular temperature of the entering particles. Figures 2 and 3 assume a value of 30 m^2/s^2 for this quantity. The solid-phase streamlines obtained for the IGT case with inlet granular temperatures of 10 m^2/s^2 and 1 m^2/s^2 are shown in Figures 5a and 5b, respectively. It is clearly seen that quantitative changes come about when this parameter is varied. The reason for this sensitivity is that the value of this parameter at the inlet dictates the rate of segregation of the particles toward the wall. Higher the granular temperature, faster is the rate of segregation. It is essential that a dense region of particles develop in the vicinity of the wall to yield downflow of particles there. At low values of inlet granular temperatures, appreciable accumulation of particles does not develop within the available riser height. A decrease in the extent of downflow with decreasing inlet granular temperature is accompanied by a decrease in the residence time of the particles (see Table 3).

Effect of inelastic particle-particle collisions

All the examples discussed above assume that the particle-particle collisions are perfectly elastic ($\gamma_1 = 0$) and neglect the effect of gas drag on pseudothermal energy ($\gamma_2 = 0$). It was reported in our earlier study on fully developed flow (Pita and Sundaresan, 1991) that with these assumptions the model yielded realistic-looking results. However, if we made the particle-particle collisions slightly inelastic, the results were altered dramatically. For the same combination of parameters and fluxes as in Figure 2, the fully developed flow pattern computed with $e = 1$ exhibited appreciable downflow solids (and gas) near the wall. When e was set to be 0.9999, the downflow disappeared altogether in *fully developed* flow. Inelastic collisions rapidly damp out the fluctuating motion of particles: the granular temperature is lowered. This then reduces the driving force for segregation of particles toward the wall. The cross-sectional average of solid volume fraction in fully developed state decreased from 0.047 to 0.0164 when the coefficient of restitution was changed from unity to 0.9999.

Figure 6 shows the results of *developing flow* calculations for the case of $e = 0.9999$. All other parameters are as in Figure 2a. A comparison of these results with fully developed flow patterns mentioned earlier reveals major differences. First, note that the recirculation still persists in developing flow (Figure 6). Second, the inventory of particles in the bed increased upon decreasing the coefficient of restitution in the present simulation, which is opposite to the trend seen in the fully developed case.

Given the above profound, unrealistic sensitivity to changes in e, one is forced to confront the question of physical relevance of the computed results. It was found in our earlier study (Pita and Sundaresan, 1991) that the fully developed flow patterns predicted with $e = 1$ agreed remarkably well with experimental data. Hence, we restrict our attention to the case of $e = 1$ in the following discussion.

Effect of exit

The computer program assumes a radial outflow at the top of the column. In all the figures presented thus far, it was assumed that this outflow region had a height of 10 cm. The sensitivity of the results to the outlet size was examined as described below. Figure 7 corresponds to an outlet opening of 20 cm (with all other quantities being the same as in Figure 2), while Figure 8 is the result of a rather constricted outlet (5 cm). It can be readily seen from a comparison of these figures that the exit opening has only a very small effect on the streamlines, particularly on the occurrence of internal recirculations. The total mass of solids in the riser tube was found to increase slightly when the exit opening was made smaller, as one would intuitively expect (see Table 3).

It is known from experiments that the exit configuration can have a profound effect on the flow patterns (Grace, 1990). The solids holdup in the riser obtained with a smooth (elbow) exit is considerably smaller than that obtained with an abrupt side exit. A reconciliation of this experimental result with our computational result is perhaps that within a given class of exit design, changes in exit dimensions will have only small effects. This point remains to be verified in a future study.

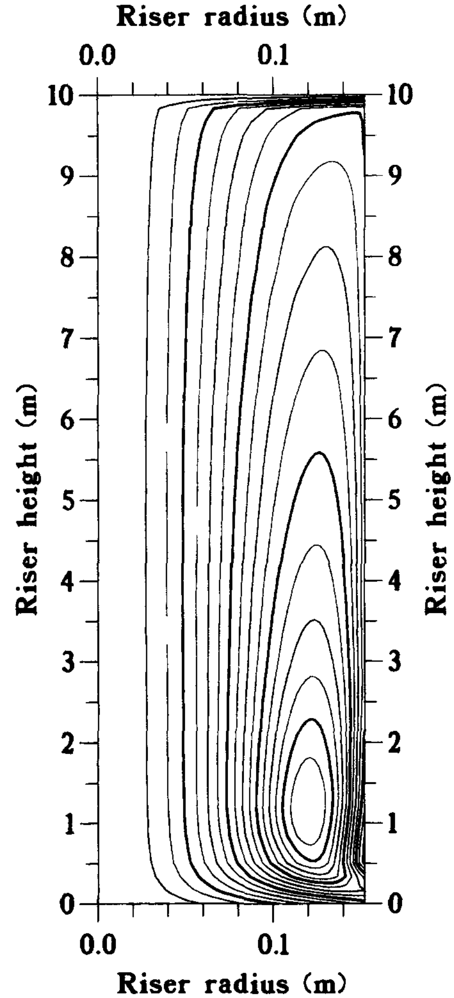

Figure 6. Effect of inelastic collisions between particles on particle phase streamlines.

Effect of riser diameter

Figure 9 presents the solid-phase streamlines obtained in a riser with a radius of 30.4 cm and an outlet of 20 cm. The fluxes are the same as in all the previous figures. This figure can be compared with Figure 7 corresponding to the same outlet height, but half the tube radius, or with Figure 2a corresponding to half the outlet size and tube radius. It is readily seen that the results obtained with a larger tube are qualitatively similar to those obtained with smaller risers.

One would intuitively expect that the lengths of the entrance and exit regions will increase upon increasing the tube radius, so that quantities such as inventory of particles in the bed should be farther away from the fully developed values in the case of wider tubes. The cross-sectional average values of solids

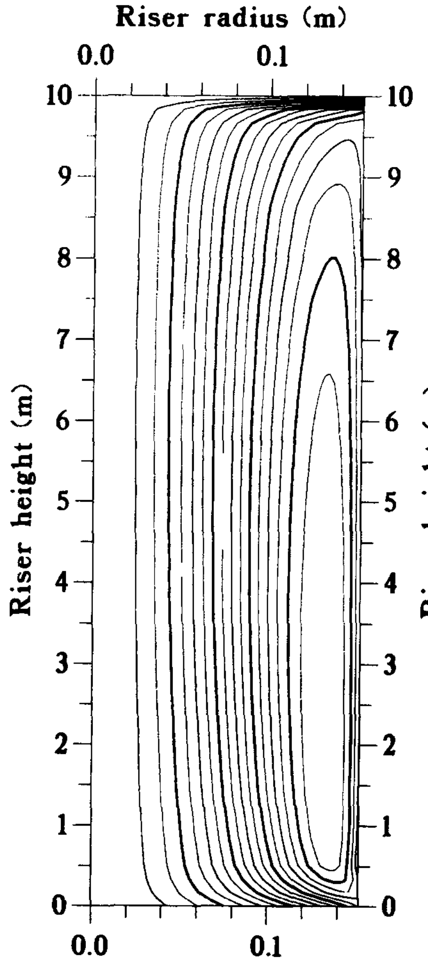

Figure 7. Effect of exit size on particle-phase streamlines.

See Tables 1 and 2 for parameter values with the exception that the outlet opening is now 20 cm wide.

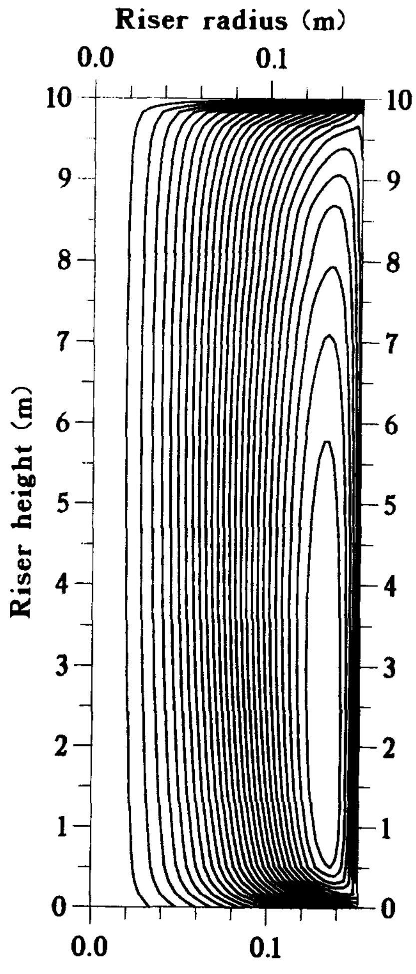

Figure 8. Effect of exit size on particle-phase streamlines.

See Tables 1 and 2 for parameter values with the exception that outlet opening is now 5 cm wide.

fraction corresponding to the fully developed state in a 30.4-cm-radius riser was found to be 0.128, which is substantially larger than the average-volume fraction in the 10-m-tall riser (see Table 3).

Core-annulus flow

Several different cases of core-annulus flow were examined. However, only two representative cases will be described here to illustrate the sort of results predicted by the model. The parameter values used in the simulations are presented in Tables 1, 2 and 4. The corresponding solid flow streamlines are presented in Figure 10a. The jet of gas entering in the core pushes the particles entering in the annular region toward the wall. However, the upward-moving particles soon encounter the particles descending in the wall region, the net effect being that both streams of particles get deflected toward the tube axis. This entire pattern of flow is consistent with what one would intuitively expect. Figure 10b presents the gas flow streamlines corresponding to this case. It is seen that the gas entering in the core region, spreads out as a fan at first. However, the recirculating gas and solid cause a compression of this fan forcing the gas to flow back towards the tube axis. The average-volume fraction of solids in the bed (see Table 3) is slightly higher than that corresponding to the fully developed cross-sectional average value of 0.047. The residence time of particles in a bed with core-annulus type of inlet is much larger than that with a uniform inlet (Table 3). Figure 11 presents the solid flow streamlines obtained with a riser of considerably larger diameter (0.5 m). All the parameter values, with the exception of riser diameter, are the same as in Figure 10. The extent of recirculation is even more pronounced in the larger diameter riser. A simple measure of the extent of recirculation is the so-called slip factor. The slip factor is defined as the ratio of the (cross-sectional) average interstitial velocities of the particles and the gas. The slip factors evaluated at a height of 5 m corresponding to these two cases are 0.448 and 0.524, respectively.

Circumferential gas injection

This mode of gas injection yielded a dramatically different

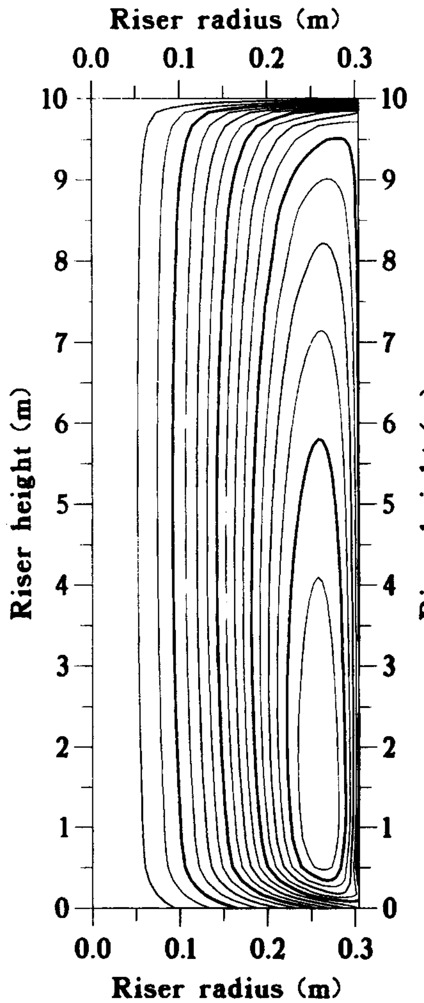

Figure 9. Effect of riser diameter on particle-phase streamlines.

See Tables 1 and 2 for parameter values with the exception that the tube radius is now 30.4 cm.

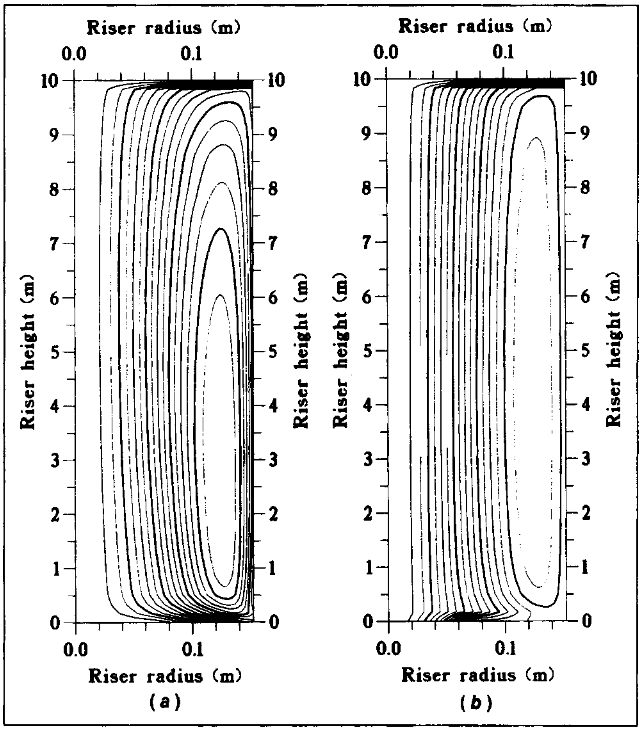

Figure 10. a. Particle-phase streamlines for core-annulus flow; b. gas-phase streamlines for core-annulus flow.

See Tables 1 and 3 for parameter values.

pattern of developing flow at the bottom of the riser. Figure 12 shows the solid flow streamlines obtained when the gas was injected horizontally (radially inward) along the circumference. The parameter values used in the simulations are summarized in Tables 1, 2, 4 and 5. To get a satisfactory resolution of the flow pattern, a much finer grid spacing was used at the bottom of the riser (than in the cases of uniform inlet and core-annulus flow), as shown in Figure 13. It is readily apparent from Figures 2a, 10a and 12 (all of which correspond to the same net gas and solid fluxes) that the inlet configuration has a profound effect on the flow development. The slip factor computed at a height of 5 m for these three cases are 0.453, 0.448, and 0.540, respectively. It is clearly seen that the circumferential injection has resulted in a decrease in the extent of particle segregation to the wall (and recirculation). It should be remarked that the very fact that the inlet configuration has a profound effect in the flow pattern in the entire riser implies that the riser is not tall enough to obtain a truly fully developed flow region. (It should also be remarked that for the net gas and solid fluxes considered in these figures, we found only a single fully developed flow solution.)

Table 4. Core-Annulus Flow

Riser Height	10 m
Riser Radius	0.152 m
Radial Outlet (at the Top) Opening	0.1 m
Core Radius	0.076 m
Inlet Solids Volume Fraction (Annulus)	0.2
Inlet Solids Axial Velocity (Annulus)	0.38 m/s
Inlet Gas Axial Velocity (Annulus)	0.48 m/s
Inlet Gas Axial Velocity (Core)	13.6 m/s
All Inlet Radial Velocities	0
Inlet Particle Temperature	20 m^2/s^2

The solid flow streamlines have peculiar shapes at the bottom of the riser for the case of circumferential injection. Calculations were performed for a number of gas and solids fluxes, and riser diameters. This pattern was found to persist. The particles are rapidly deflected toward the tube axis by the jet of gas injected circumferentially, thus creating a region of high solid volume fraction near the tube axis. Once the particles move up past this jet, the strong radial gradient particle phase pressure causes the streamlines to fan out to the wall. At some further height, the streamlines deflect back toward the axis, and this is clearly due to the downward-moving particles in the wall region.

The effect of the angle of inclination of the injection nozzles was also examined. Figure 14 presents the solids flow streamlines obtained with an injection angle of 45 degrees (with all the other quantities being as in Figure 12). It appears that the angle of inclination has only a small effect.

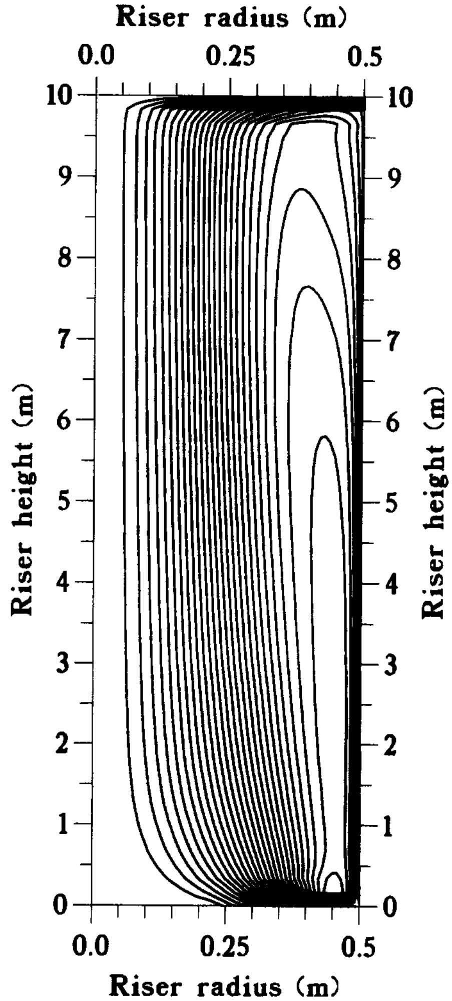

Figure 11. Particle-phase streamlines.

See Tables 1 and 3 for parameter values with the exception that tube radius is now 50 cm.

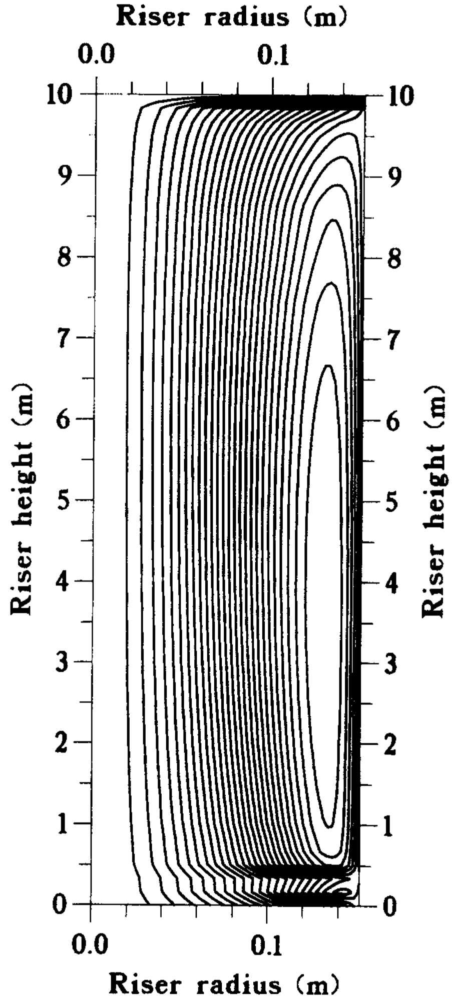

Figure 12. Particle-phase streamlines for circumferential gas injection.

See Tables 1 and 4 for parameter values for horizontal gas injection.

Summary

The steady, developing flow of a gas-solid mixture in a vertical cylindrical riser has been studied. To simplify the analysis, inlet and exit configurations were chosen to permit the assumption of cylindrical symmetry. Three different inlet configurations were examined.

Focusing first on the simplest case of uniform inlet in the bottom, the evolution of flow streamlines and solid segregation to the wall are illustrated. The internal recirculation of solids and gas evolves as a result of the segregation of particles to the wall.

A core-annulus type of inlet configuration, in which a gas-solid mixture enters in the annular region and a jet of gas is introduced in the core, has also been analyzed. This type of inlet configuration promotes internal recirculation.

The third case examined in this study is concerned with the effect of circumferential gas injection on the manner in which the flow develops. It was found that the segregation of particles to the wall occurred more slowly in this case. This resulted in a drastic reduction in the recirculation of solids in the examples analyzed. Such a recirculation is believed to be undesirable in reactor applications.

It is needless to emphasize that real gas-solid flow in risers is inherently unsteady, while our analysis is a steady-state simulation. It would be helpful to have experimental data on developing flows to compare with model prediction, but such data are not available. Thus, the only conclusion that can be drawn at the present time is that the qualitative trends predicted

Table 5. Circumferential Injection

Riser Height	10 m
Riser Radius	0.152 m
Radial Outlet (at the Top) Opening	0.1 m
Bottom Uniform Inlet	
Inlet Solids Volume Fraction	0.2
Inlet Solids Axial Velocity	0.2858 m/s
Inlet Gas Axial Velocity	0.3858 m/s
Inlet Particle Temperature	30 m^2/s^2
Circumferential Injection of Gas	
Radial (Inward) Velocity	2.62 m/s
Inlet Opening	0.1 m

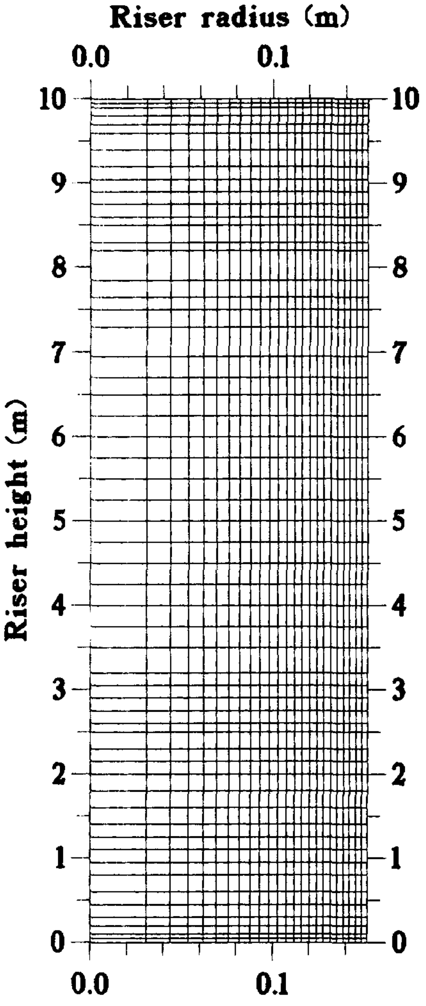

Figure 13. Finite difference grid used to simulate the case of circumferential gas injection.

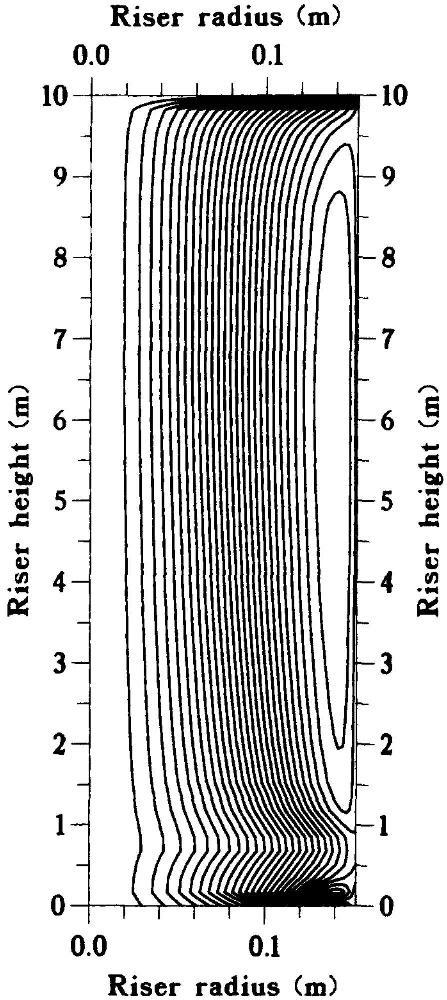

Figure 14. Particle-phase streamlines for circumferential gas injection.

Angle of injection is 45°.

by the model are realistic. The large effect that inlet configuration can have on the pattern of flow development has been recorded by Saxton and Worley (1970). This is indeed seen in our simulations. The present analysis suggests that circumferential injection of gas can decrease the extent of internal recirculation in riser tubes.

Acknowledgment

We would like to acknowledge many helpful discussions with F. J. Krambeck, A. A. Avidan, and D. L. Johnson in preparing this article. We also thank Cray Research Inc. for granting us access to their YMP-8 multiprocessor in Eagan, MN, especially Verrill Rinehart for her technical assistance.

Notation

C_d = drag coefficient, Eq. 12
d_s = particle diameter, m
e = coefficient of restitution for particle-particle collisions
e_w = coefficient of restitution for particle-wall collisions
f_1 = effective viscosity of the particle phase, Eq. 8
f_2 = effective pseudothermal conductivity, Eq. 9
g = acceleration due to gravity, m/s^2
g_o = radial distribution function
m = mass of a single particle, kg
P = gas pressure, kPa
$\underline{q}_{pt}$ = pseudothermal energy flux, kg/s^3, Eqs. 4 and 6
r = radial coordinate
R_t = tube radius
$\underline{\underline{S}}$ = particle phase stress tensor, kg/m·s^2
U_g, $\overline{U}_s$ = local average velocities of gas and particles, m/s

Greek letters

β_{sg} = drag coefficient defined by Eq. 10
γ_1 = rate of dissipation of pseudothermal energy by inelastic collisions between particles, Eq. 7, kg/m·s^3
γ_2 = rate of dissipation of pseudothermal energy by gas drag, Eq. 11, kg/m·s^3
ϵ_g, ϵ_s = local average volume fractions of gas and solid, $\epsilon_g + \epsilon_s = 1$
ϵ_o = maximum solid volume fraction
θ = granular (or particle) temperature, m^2/s^2
η, λ, μ, μ_b = terms defined immediately after Eq. 11
μ_g = viscosity of gas, kg/m·s
ρ_g, ρ_s = density of gas and solid, kg/m^3
$\underline{\underline{\sigma}}$ = stress tensor associated with the particle assembly, defined in a compressive sense, Eq. 5
ϕ^1 = specularity coefficient for particle-wall collisions

Literature Cited

Adewani, M., and H. Arastoopour, "Two-Dimensional Steady State Hydrodynamic Analysis of Gas-Solids Flow in Vertical Pneumatic Conveying Systems," *Powder Tech.*, **48**, 67 (1986).

Anderson, T. B., and R. Jackson, "A Fluid Mechanical Description of Fluidized Beds: Equations of Motion," *Ind. Eng. Chem. Fundam.*, **6**, 527 (1967).

Arastoopour, H., and C. Cutchen, "Measurement and Analysis of Particle-Particle Interaction in a Cocurrent Flow of Particles in a Dilute Gas-Solids System," *Chem. Eng. Sci.*, **40**, 1135 (1985).

Arastoopour, H., and D. Gidaspow, "Vertical Pneumatic Conveying Using Four Hydrodynamic Models," *Ind. Eng. Chem. Fundam.*, **18**, 123 (1979a).

Arastoopour, H., and D. Gidaspow, "Analysis of IGT Pneumatic Conveying Data and Fast Fluidization Using a Thermohydrodynamic Model," *Powder Tech.*, **22**, 77 (1979b).

Arastoopour, H., C. Wang, and S. Weil, "Particle-Particle Interaction Force in a Dilute Gas-Solids System," *Chem. Eng. Sci*,. **37**, 1379 (1982).

Bader, R., J. Findlay, and T. M. Knowlton, "Gas/Solid Flow Patterns on a 30.5-cm-Diameter Circulating Fluidized Bed," *Int. Circulating Fluidized-Bed Conf.*, Compiegne, France (Mar. 14-18, 1988).

Bartholomew, R., and R. Casagrande, "Measuring Solids Concentration in Fluidized Systems by Gamma-Ray Absorption," *Ind. Eng. Chem.*, **49**, 428 (1957).

Chen, Y.-M., S. Rangachari, and R. Jackson, "A Theoretical and Experimental Investigation of Flow in a Vertical Standpipe," *Ind. Eng. Chem. Fundam.*, **23**, 354 (1984).

Ding, J., and D. Gidaspow, "A Bubbling Fluidization Model Using Kinetic Theory of Granular Flow," *AIChE J.*, **36**, 523 (1990).

Gidaspow, D., and C. Solbrig, "Transient Two Phase Flow Models in Energy Production," AIChE Meeting (1976).

Ginestra, J. C., S. Rangachari, and R. Jackson, "A One-Dimensional Theory of Flow in Vertical Standpipes," *Powder Technol.*, **27**, 69 (1980).

Grace, J. R., "High-Velocity Fluidized Bed Reactors," *Chem. Eng. Sci.*, **45**, 1953 (1990).

Hinze, J., "Momentum and Mechanical Energy Balance Equations for a Flowing Homogeneous Suspension with Slip Between the Two Phases," *Appl. Sci. Res.*, **11**, 33 (1962).

Hui, K., P. K. Haff, J. E. Ungar, and R. Jackson, "Boundary Conditions for High-Shear Grain Flows," *J. Fluid Mech.*, **145**, 223 (1984).

Jenkins, J. T., "Rapid Flow of Granular Materials," *Non-Classical Continuum Mechanics: Abstract Techniques and Applications*, R. J. Kops and A. A. Lacey, eds., p. 213, Cambridge University Press (1987).

Johnson, P. C., and R. Jackson, "Frictional-Collisional Constitutive Relations for Granular Materials with Application to Plane Shearing," *J. Fluid Mech.*, **176**, 67 (1987).

Leung, L. S., and P. Jones, "Coexistence of Fluidized Solids Flow and Packed Flow in Standpipes," *Proc. Int. Fluidization Conf.*, **116**, Cambridge University Press (1978).

Louge, M., E. Mastorakos, and J. T. Jenkins, "The Role of Particle Collisions in Pneumatic Transport," *J. Fluid Mech.*, **231**, 345 (1991).

Lun, C., S. B. Savage, D. Jeffrey, and N. Chepurniy, "Kinetic Theories for Granular Flow: Inelastic Particles in Couette Flow and Slightly Inelastic Particles in a General Flow Field," *J. Fluid Mech.*, **140**, 223 (1984).

Mountziaris, T. J., and R. Jackson, "The Effects of Aeration on the Gravity Flow of Particles and Gas in Vertical Standpipes," *Chem. Eng. Sci.*, **46**, 381 (1991).

Pita, J. A., and S. Sundaresan, "Gas-Solid Flow in Vertical Tubes," *AIChE J.*, **37**, 1009 (1991).

Saxton, A., and A. Worley, "Modern Catalytic Cracking Design," *Oil and Gas J.*, **68**, 82 (1970).

Sinclair, J. L., and R. Jackson, "The Effect of Particle-Particle Interactions on the Flow of Gas and Particles in a Vertical Pipe," *AIChE J.*, **35**, 1473 (1989).

Tsuo, Y. P., and D. Gidaspow, "Computation of Flow Patterns in Circulating Fluidized Beds," *AIChE J.*, **36**, 885 (1990).

Weinstein, H., M. Shao, and L. Wasserzug, "Radial Solid Density Variation in a Fast-Fluidized Bed," *AIChE Symp. Ser.*, **80**, 117 (1984).

Yerushalmi, J., and A. A. Avidan, "High Velocity Fluidization," *Fluidization*, 2nd ed., J. F. Davidson, R. Clift, and D. Harrison, eds., Academic Press, p. 225 (1985).

Yerushalmi, J., N. Cankurt, D. Geldart, and B. Liss, "Flow Regimes in Vertical Gas-Solid Contact Systems," *AIChE Symp. Ser.*, **74**, 1 (1978).

Youchou, L., and M. Kwauk, "The Dynamics of Fast Fluidization," *Fluidization*, J. Grace and J. Matsen, eds., Plenum Press, New York (1980).

Manuscript received June 10, 1992, and revision received Oct. 5, 1992.